M51 - Fully-sampled Aperture Synthesis Maps of CO Emission

K.Y. Lo, D.S. Adler, R.J. Allen, R. Plante
Astronomy Department, University of Illinois
M.C.H. Wright
Radio Astronomy Lab, University of California, Berkeley
G. Rydbeck
Onsala Space Observatory

ABSTRACT. We present aperture synthesis CO maps of two 2'-fields of M51. These maps, in contrast to previous interferometer maps, do not have any missing flux. They show directly that most of the CO emission arise from broad spiral arms, whereas previously it was assumed that the missing CO flux ($\geq 65\%$ of the total flux) is uniformly distributed. Inferences involving extended CO emission and widths of the CO spiral arms based on interferometer maps with missing flux may need to be reviewed. The "missing short spacings" problem is also discussed.

1. Introduction

For M51 (and spiral galaxies generally), one of the important issues is to determine the relative distribution of CO emission in spiral arms and in between arms, because this has bearings on the formation and the life-time of molecular clouds. This requires CO maps with sufficiently high resolution, best obtained by using millimeter-wave interferometers. However, all interferometer maps of CO emission from galaxies suffer from the "missing short spacings" problem.

An interferometer map can only present the small scale sturctures such as the peaks and ridges in the brightness distribution. Such maps are excellent for displaying small scale structure not otherwise possible. However, when interpretations of the results involve the extended components, which are not sampled by the interferometer, such maps have to be viewed with caution. In particular, the "missing short spacings" problem affects interferometer CO maps of M51, which contain a small fraction (≤ 0.35) of the flux within the primary field of view (Lo *et al.* 1987-L87; Vogel *et al.* 1988-VKS; Rand and Kulkarni 1990-RK).

With the recent completion of several millimeter-wave interferometers around the world, interferometer maps of molecular emission from galaxies will be increasingly common. It is therefore very important for the general astronomer to understand the "missing short spacings" problem in order to interpret interferometer maps properly.

2. Missing Short Spacings and Moment Maps

The antennas of an interferometer are usually placed no closer than $\sqrt{2}$D apart to avoid collisions, where D is the diameter of the individual antenna. As a result, there is a region around the origin of the uv-plane with a radius $\leq D/\lambda$ where the visibilities cannot be measured by the interferometer (for the basic principles of aperture synthesis, see Thompson *et al.* 1986). If the source has a lot of structure with angular sizes $\geq \lambda/2D$, the visibility amplitudes will be large in exactly the region of the uv-plane where the interferometer cannot probe.

F. Combes and F. Casoli (eds.), Dynamics of Galaxies and Their Molecular Cloud Distributions, 81–85.

This results in "dirty" maps in which large scale structures have been filtered out and regions of negative intensity surround where the small scale structures are. Furthermore, given the typically low signal to noise ratios (S/N) in maps of CO emission from galaxies, the deconvolution process to derive the "clean" maps, which are the ones presented and used for analysis, requires close inspection and can be very subjective.

Another aspect of interferometric maps of extragalactic CO that requires comment is the way the integrated intensity maps are derived. The integrated intensity maps that have been presented are not simple sums of the maps at each velocity bin (channel maps), although this is not usually stated explicitly. A simple sum of M channel maps will yield an integrated map with noise that has a variance M times σ, the noise variance of each channel map. Since there is not usually signal in every channel at the same spatial location, the S/N of the summed map will be reduced from that of the individual channel maps.

The integrated intensity maps are usually the "zeroth moment" maps derived by the "masked moment" method which was originally developed for 21 cm HI maps of galaxies that also suffer from limited S/N. Consider a data cube, $T(x, y, v_i)$, made up of the channel maps, $T_i(x, y)$. The "zeroth moment" map is calculated by

$$M_0(x, y) = \sum_i T_i(x, y),$$

but the inclusion of $T_i(x, y)$ *in the sum depends on a conditional test.* $T_i(x, y)$ is included in the sum if $\langle T_i(x, y)\rangle$ is greater than a threshold value, ususally set about equal to σ. $\langle T_i(x, y)\rangle$ is the averaged value of $T_i(x, y)$ in a small volume around the pixel (x, y, v_i) that should contain more than one resolution element in the spatial and velocity dimensions. Both the threshold value and the volume are specified inputs to the moment calculation. This conditional test tends to exclude from the zeroth moment map pixels that contain noise *and* pixels that contain low level signal with magnitudes comparable to the noise. *The noise statistics in such a moment map is no longer straightforward.*

3. Observations and Results

To obtain fully sampled CO maps in M51, we combined the short spacing visibilities derived from observations with the Onsala Space Observatory (OSO) 20-m telescope with the visibilities from the Berkeley-Illinois-Maryland millimeter array (BIMA). BIMA was used to observe two fields of M51. The half-power primary beam-width (HPBW) is 110" at 115 GHz. Eighteen different baselines ranging from 8 to 73 meters provide a relatively uniform uv coverage, and result in a synthesized beam size of 7" x 11" (350 pc x 550 pc at a distance of 10 Mpc). The spectrometer was set up for maximum velocity coverage of 750 km/sec (an effective bandwidth of 290 MHz), centered on v_{LSR}=470 km/sec with a resolution of 3.25 km/sec. The data were averaged to a resolution of 10.4 km/sec before the channel maps were produced using natural weighting.

Single dish spectra of the CO (J=1–0) line from M51 were obtained using the OSO 20-m (Rydbeck *et al.* 1985-RHR; Rydbeck *et al.* 1989-RHWR), with a HPBW of 33". Spectra were obtained at points 20" apart, although some regions are sampled at a spacing of 11". An area larger than the two 2'-fields was mapped. The method used to combine the single-dish and interferometer data is similar to that described by Vogel *et al.* (1984) and is described in more detail in Adler *et al.* (1990).

Figure 1 shows the CO spectra (flux density versus velocity) of field 1 derived from the single-dish, interferometer, and combined data sets. The combined data set recovers > 90% of the total flux density at all velocities, and maps with BIMA observations alone recover 30–95% of the flux. Interferometer maps obtained with 10-m antennas typically recovers 25–35% of

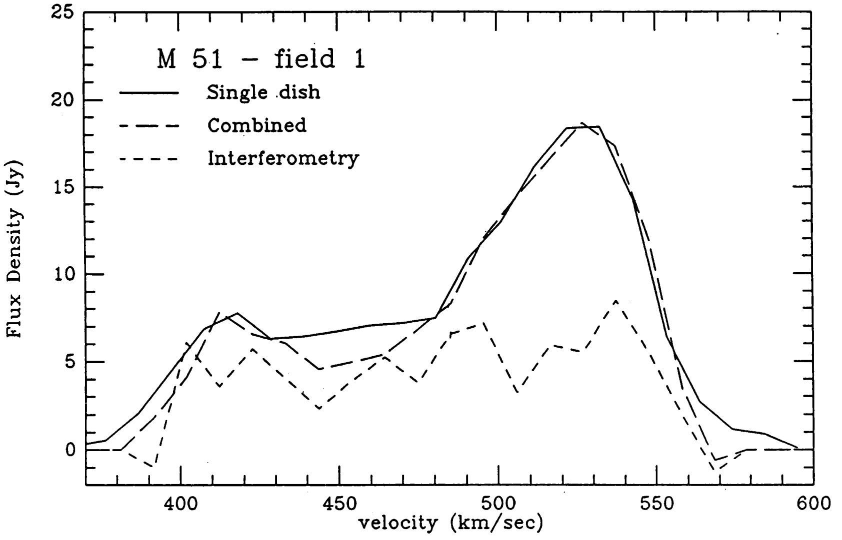

Fig. 1

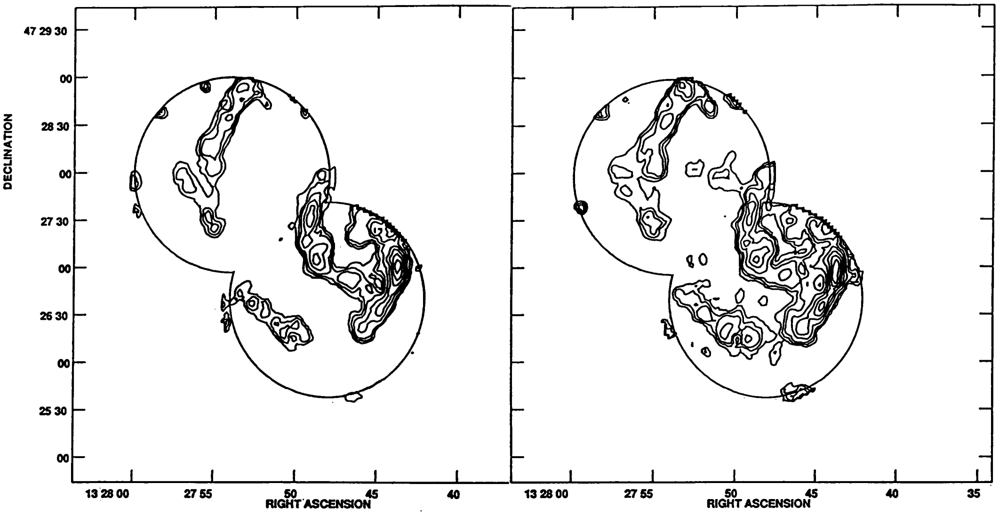

Fig. 2

Fig. 3

https://doi.org/10.1017/S0074180900243593 Published online by Cambridge University Press

the single-dish flux in their M51 surveys (L87, VKS, RK). Because the BIMA antennas have diameters of 6-m and the missing short spacings are correspondingly shorter, the BIMA maps are more sensitive to large-scale structure and recover a larger fraction of the total flux density.

The mosaiced integrated intensity maps for the two 2'-fields are shown in figures 2 (BIMA only) and 3 (combined). They are "zeroth moment" maps, for which the threshold was set equal to $\sigma \sim 0.3$ Jy/beam, the velocity channels were Hanning smoothed, and the spatial pixels were Gaussian smoothed over 10". The moment maps were then corrected for the primary beam response and mosaiced together using a simple weighting technique that takes into account a cell's position relative to the phase center of the field (Mundy, *et al.* 1986; VKS).

4. Discussion

The combined maps show that the bulk of the recovered flux is found in the arms, making them *wider and more extended* than the CO arms shown in previous interferometer maps. Thus, comparisons of the CO distribution to other tracers of spiral structure will need to be reviewed. The usual assumption has been that the missing flux in such maps is distributed uniformly throughout the field of view (L87, VKS, RK). Some inter-arm CO emission is seen in the combined map, especially in the nuclear region and between the inner and outer arms. But overall, the map does not show a significant amount of inter-arm CO emission. The lowest contour of the integrated intensity map is 7.5 (Jy/beam)-km/sec or 9.4 K-km/s. This sets an upper limit to the peak CO intensity for any inter-arm CO emission, and the very small fraction of flux density not accounted for in the spiral arms sets an upper limit to the total amount of inter-arm CO emission.

The *peak* arm-to-inter-arm CO intensity contrast is $>16:1$, similar to those drived from a 12" resolution CO(J=2–1) map obtained with the IRAM 30-m telescope (Guelin *et al.* 1989-G89; Garcia-Burrillo *et al.* 1990-G90). Such high *peak* CO intensity contrast ratio is similar to that observed in M31 (Stark 1985). If we compare the CO intensity averaged along a spiral arm to the the inter-arm intensty, we get a ratio of 4.6:1 for the 2 fields we observed. Such averaged intensity ratios are similar with those derived from previous single-dish observations of the molecular gas in M51 ($\geq$5:1 RHWR; 4:1 Verter and Kutner 1988).

Whether the CO intensity arm-to-inter-arm contrast ratio can be equated to the contrast ratio of the molecular hydrogen column density, $N(H_2)$, is not clear. Independent of the physics involved, empirically the intensity contrast ratio in M51 is different, depending on which of the CO(1-0), CO(2-1) or ^{13}CO lines is used (G89, G90). Apparently, much more work is needed before any definitive statements can be made about the arm-to-inter-arm contrast in $N(H_2)$. Statements on the contrast ratio of star formation efficiency (SFE, usually *assumed* to be the ratio of $H\alpha$ flux to CO intensity) may be further complicated by the lack of $H\alpha$ maps with high dynamic range and by the extinction across the face of the galaxy.

Regions of figure 3 were reproduced with higher velocity resolution (3.5 km/sec) to check for velocity gradients in the gas distribution. Slices perpendicular to the spiral arms produced profiles that are very similar to those found in N-body spiral density wave models (Roberts and Hausman 1984; Roberts and Adler 1989). Profiles with velocity dips of up to 30 km/sec are seen in the inner arms. The similarity of these profiles to those of the N-body density-wave models indicates that strong density-waves are present in the arms of M51.

The work summarised here is reported in more detail in Adler *et al.* (1990). Financial support for the work is from the US National Science Foundation and the University of Illinois.

References

Adler, D.S., Lo, K.Y., Wright, M.C.H., Rydbeck, G., Plante, R.L., and Allen, R.J. 1990, Astrophys. J., submitted.

Garcia-Burillo, S *et al.* , 1990, this volume.

Guelin, M., Garcia-Burillo, S., Blundell, R., Cernicharo, J., Despois, D., and Steepe, H. 1989, Highlights of Astronomy, Volume 8, D. McNally ed., IAU, page 575 (G89).

Lo, K.Y., Ball, R., Masson, C.R., Phillips, T.G., Scott, S., and Woody, D.P. 1987, Astrophys. J. Letters, 317, L63 (L87).

Mundy, L.G., Scoville, N.Z., Baath, L.B., Masson, C.R., and Woody, D.G. 1986, Astrophys. J. Letters, 304, L51.

Rand, R.J., and Kulkarni,S.R. 1990, Astrophys. J. Letters, 349, L43 (RK).

Roberts, W.W., and Adler, D.S. 1989, Celestial Mechanics, 45, 285.

Roberts, W.W., and Hausman, M.A. 1984, Astrophys. J., 277, 144.

Rydbeck, G., Hjalmarson, A., and Rydbeck, O.E.H. 1985, Astron. Astrophys, 144, 282 (RHR).

Rydbeck, G., Hjalmarson, A., Wilkind, T., and Rydbeck, O.E.H. 1989, in the Proceedings of the UMASS Conference on Molecular Clouds in the Milky Way and External Galaxies, J. Dickman, R. Snell and J. Young eds., Springer Verlag, Berlin, page 446 (RHWR).

Stark, A.A. 1985, in "The Milky Way Galaxy", H. van Woerden ed., IAU, page 445.

Thompson, R., Moran, J. M., Swenson, G., 1986, "Interferometry and Synthesis in Radio Astronomy", Wiley, New York.

Verter, F., and Kutner, M.L. 1988, Lecture Notes in Physics - "The Outer Galaxy", Vol 306, L. Blitz and F.J. Lockman eds., Springer Verlag, Berlin, page 253.

Vogel, S.N., Kulkarni, S.R., and Scoville, N.Z. 1988, Nature, 334, 402 (VKS).

Vogel, S.N., Wright, M.C.H., Plambeck, P.L., and Welch, W.J. 1984, Astrophys. J., 283, 655.